

How to test path-length dependence in energy-loss mechanisms: Analysis leading to a new observable

Magdalena Djordjevic,^{1,*} Dusan Zigic,¹ Marko Djordjevic,² and Jussi Auvinen¹

¹*Institute of Physics Belgrade, University of Belgrade, Serbia*

²*Faculty of Biology, University of Belgrade, Serbia*



(Received 17 November 2018; published 19 June 2019)

When traversing the QCD medium, high- p_{\perp} partons lose energy, which is typically measured by suppression, and predicted by various energy-loss models. A crucial test of different energy-loss mechanisms is their functional dependence on the length of traversed medium (i.e., path-length dependence). The upcoming experimental measurements will, for the first time, generate data that may allow to clearly assess this dependence, in particular, by comparing results from Pb + Pb collisions with future measurements in smaller systems. However, to perform such a test, it is crucial to choose an optimal observable. To address this, we here use both analytical and numerical analyses to propose a novel—simple, yet accurate and robust—observable for assessing the path-length dependence of the energy loss. Our numerical results show that, by using this observable, different (underlying) energy-loss mechanisms may be directly differentiated from the experimental data, which is, in turn, crucial for understanding the properties of the created QCD medium.

DOI: [10.1103/PhysRevC.99.061902](https://doi.org/10.1103/PhysRevC.99.061902)

Introduction. Understanding properties of quark-gluon plasma (QGP) [1] created at the Large Hadron Collider (LHC) and Relativistic Heavy Ion Collider (RHIC) experiments is a major goal of ultrarelativistic heavy ion physics [2], which would allow understanding properties of QCD matter at its most basic level. Energy loss of high- p_{\perp} partons traversing this medium is an excellent probe of its properties [3], which provided a crucial contribution [2] to establishing that QGP is created in these experiments. Comparing predictions of different energy-loss models [4], and, consequently, different underlying energy-loss mechanisms with experimental data is, therefore, crucial for understanding properties of created QGP. However, an open question is how to provide the most direct comparison of energy-loss predictions with experimental data.

The most basic signature for distinguishing different energy-loss models is how the predicted energy loss depends on the length of the traversed QCD medium (so-called path-length dependence). This path-length dependence directly relates to different underlying energy-loss mechanisms, such as perturbative QCD collisional (with typically linear [5,6]), radiative (with typically quadratic [7–11]), or alternatively conformal anti-De Sitter holography models (with third-power [12] energy-loss path-length dependence). Moreover, even in such cases, the division is not so clear as there are numerous other effects that can significantly alter these path-length dependencies [13–15]: inclusion of the mass of the leading particle, finite-size, and finite temperature effects in QGP, interference effects, etc. Therefore, accurately assessing the path-length dependence is also crucial for understanding

mechanisms that underly the observed energy loss, which is, in turn, necessary for investigating the properties of QCD matter created at RHIC and LHC, i.e., for precision QGP tomography.

However, despite its essential importance and longstanding interest in this subject, it is still not possible to directly infer the energy-loss path-length dependence from experimental measurements and, consequently, provide a possibility to discriminate between different energy-loss models. To our knowledge, the most comprehensive study in this subject [16,17], attempted to extract the energy-loss path-length dependence from a thorough simultaneous study of R_{AA} and v_2 predictions and data (at Au + Au collisions at RHIC and Pb + Pb collisions at the LHC) but was not able to constrain this dependence based on the existing observables and data. With this in mind, the goal of this Rapid Communication is to propose a novel approach for extracting the energy-loss path-length dependence.

It is intuitively clear that the most direct probe of the path-length dependence would involve comparing experimental data (and the related theoretical predictions) for two-collision systems of different sizes. Moreover, it would be optimal if the size would be the only property distinguishing these two systems, i.e., that other properties and parameters needed for generating relevant predictions would be the same between the two systems. Equally important, it is necessary to propose an appropriate observable from which the path-length dependence can be reliably extracted. Consequently, the aim of the analysis presented in this Rapid Communication is to infer an optimal system and an optimal observable for assessing the energy-loss path-length dependence. We will also test how reliable and robust is the inferred observable to different types of energy loss, probes, centralities, and collision systems.

* magda@ipb.ac.rs

Appropriate observable. In this section, we first start by asking what is an appropriate observable to assess the energy-loss path-length dependence? To start addressing this question, we note that such an observable should be sensitive to jet-medium interactions (so that energy-loss path-length dependence can be reliably extracted). On the other hand, it should not be sensitive to the medium evolution as the details of the medium evolution would, for such a purpose, present an unwanted background. Keeping this in mind, it is evident that such an observable should be a function of R_{AA} since R_{AA} has exactly these desired properties—i.e., it is highly sensitive to the energy-loss mechanisms in QGP [18,19], whereas being insensitive to the medium evolution (i.e., it can be characterized by mean QGP temperature) [19]. The medium evolution insensitivity is also consistent with our recent result [20] of almost identical R_{AA} for constant medium temperature and (1 + 1)-dimensional Bjorken expansion; however, this still remains to be further verified by using more realistic medium evolution calculations, including event-by-event fluctuations [17,21].

Appropriate systems. Measurements for 5.02-TeV Pb + Pb collisions are available, whereas precision measurements for 5.44-TeV smaller systems (Xe + Xe, Kr + Kr, Ar + Ar, and O + O) will become available in the future with the planned beam size scan (BSS) at the LHC. As these systems have similar collision energies but different sizes (atomic mass numbers are $A = 208, 129, 78, 40, 16$ for Pb, Xe, Kr, Ar, and O), comparison of Pb + Pb with smaller systems appears to be a good candidate for the path-length dependence study. Note that the BSS at the LHC is complementary to the current beam energy scan (BES) at RHIC, as in the BES, the systems of the same size but different collision energies are tested, whereas in the BSS, the systems of the same energy but different sizes will be explored, thus providing a crucial insight in how properties of the created matter depend on the size of the colliding ions.

Computational framework. In this Rapid Communication, the R_{AA} predictions will be generated by our full-fledged numerical procedure, recently developed in Ref. [22]. The procedure is based on our state-of-the-art dynamical energy-loss formalism [5,15], which contains different important effects (some of which are unique to this model): (i) *Finite-size finite temperature* QGP, consisting of *dynamical* (that is moving) constituents. This abolishes the widely used approximations of static scattering centers, vacuumlike propagators, and/or infinite-size QGP (e.g., Refs. [7,8,10,11]). (ii) Our calculations are based on the finite temperature generalized hard-thermal-loop approach [23] in which the infrared divergencies are naturally regulated [15]. (iii) Both collisional [5] and radiative [15] energy losses are computed under *the same* theoretical framework, which is applicable to *both light and heavy flavor*. (iv) The model is generalized to the case of finite magnetic mass [24] and running coupling [25]; recently, we also applied first steps towards removing widely used soft-gluon approximation [26]. Moreover, in Ref. [18], we showed that all these ingredients are necessary for accurately explaining the high- p_{\perp} parton-medium interactions in QGP.

To generate the final medium modified distribution of high- p_{\perp} hadrons, the formalism was integrated into fully optimized numerical framework DREENA [22], which integrates the

initial- p_{\perp} distribution of leading partons [27], energy loss with multigluon [28], and path-length [29] fluctuations and fragmentation functions [30]. To generate R_{AA} predictions for Pb + Pb collisions, we use the set of parameters specified in Ref. [22], which correspond to standard literature values (not repeated here for brevity).

The dynamical energy-loss formalism was previously used to obtain a comprehensive set of R_{AA} predictions at the RHIC and LHC [22]; it shows wide agreement with the existing data [25], explaining puzzling data and generating nonintuitive predictions for future experiments [31,32] (some of which were already confirmed by subsequent data [33,34]). This then strongly indicates that our formalism can realistically describe high- p_{\perp} parton-medium interactions and that it provides a suitable framework for the goal that we want to achieve in this Rapid Communication.

Smaller systems. For R_{AA} predictions in smaller systems and their comparison with Pb + Pb collisions, one should note that R_{AA} depends on: (i) initial distribution of high- p_{\perp} partons, (ii) average temperature of the created QGP, and (iii) path-length distributions. Regarding initial distributions, we previously showed [31] that, when the collision energy is changed almost two times (from 2.76 to 5.02 TeV), the influence of the change in p_{\perp} distributions leads to only a small change (less than 10%) in the resulting suppression. Consequently, for the increase of less than 10% in the collision energy (from 5.02 to 5.44 TeV), the same high- p_{\perp} distributions can be assumed. The average temperature (\bar{T}) for each centrality region in 5.02-TeV Pb + Pb collisions is estimated according to Ref. [22]. Note that \bar{T} is directly proportional to the charged multiplicity, whereas inversely proportional to the overlap area and average size of the medium, i.e., $\bar{T} = \left(\frac{dN_{ch}/d\eta}{A_{\perp}L}\right)^{1/3}$ [22,35]. To estimate \bar{T} in smaller systems, we note that, for each centrality region, all the above quantities change in the two-collision systems: $A_{\perp} \sim A^{2/3}$; $\bar{L} \sim A^{1/3}$ [36,37]; $dN_{ch}/d\eta \sim N_{part}$, where $N_{part} \sim A$ since, for the same collision energy, $\frac{dN_{ch}/d\eta}{N_{part}}$ should remain constant with decreasing the systems' size [38,39]. This therefore leads to $\bar{T} \sim \left(\frac{A}{A^{2/3}A^{1/3}}\right)^{1/3} \sim \text{const}$, i.e., we expect that, for a fixed centrality region, \bar{T} will remain unchanged when moving from large Pb + Pb to smaller systems. Finally, the path-length distributions for smaller systems, at different centralities, can be calculated in the same manner as previously for Pb + Pb [22]. It is straightforward to see that the two distributions are similar up to a rescaling factor corresponding to $A^{1/3}$. Consequently, we see that comparison of Pb + Pb with smaller systems is, in fact, close to ideal when it comes to probing the path-length dependencies.

R_{AA} ratio. The next question is what is the exact variable (i.e., its functional dependence on R_{AA}) that should be compared for the two systems in order to extract the path-length dependence. Since R_{AA} increases when the system size decreases, it may seem that the ratio of R_{AA} for the two systems is a natural choice [40]. To test this proposal, in Fig. 1, we show momentum dependence of the R_{AA} ratio for the Xe + Xe and Pb + Pb systems (note that, for easier reading, we will first concentrate on Xe + Xe and Pb + Pb and we will

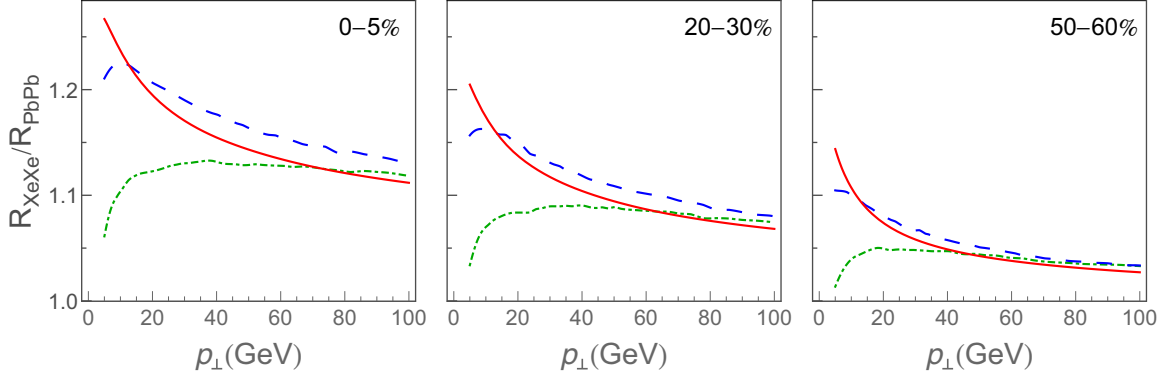


FIG. 1. Ratio of R_{XeXe} and R_{PbPb} is shown as a function of p_{\perp} for charged hadrons, D and B mesons (full, dashed, and dot-dashed curves, respectively). Centrality regions are denoted in the upper right corners of each panel.

discuss smaller systems subsequently). We see that it would be very hard to extract the path-length dependence from such a ratio, e.g., for high p_{\perp} , this ratio approaches 1, naively suggesting that the underlying model has no (or only weak) path-length dependence. However, the dynamical energy-loss model has, in fact, a strong (between linear and quadratic) path-length dependence. The same problem would emerge if experimental data would be plotted in that way, i.e., one may naively conclude that high- p_{\perp} suppression does not depend on the system size. Moreover, we see that this quantity is not robust with respect to the changes in collision centrality, which would further complicate extracting the path-length dependence from simple R_{AA} ratio.

The problem above can be intuitively understood by using scaling arguments. Fractional energy-loss $\Delta E/E$ can be estimated as [22]

$$\Delta E/E \approx \chi \bar{T}^a \bar{L}^b, \quad (1)$$

where a, b are proportionality factors, \bar{T} is the average temperature of the medium, \bar{L} is the average path-length traversed by the jet, and χ is a proportionality factor (which depends on initial jet p_{\perp}). $b \rightarrow 1$ corresponds to the linear, whereas $b \rightarrow 2$ corresponds to the quadratic [Landau-Pomeranchuk-Migdal- (LPM-) like] dependence of the energy loss.

If $\Delta E/E$ is small (i.e., for higher p_{\perp} of the initial jet, and for higher centralities), we can make the following estimate [22]:

$$R_{AA} \approx 1 - \xi \bar{T}^a \bar{L}^b, \quad (2)$$

where $\xi = (n-2)\chi/2$ and n is the steepness of the initial momentum distribution function.

The ratio of R_{XeXe} and R_{PbPb} then becomes

$$\frac{R_{XeXe}}{R_{PbPb}} \approx 1 + \xi \bar{T}^a \bar{L}^b \left[1 - \left(\frac{A_{Xe}}{A_{Pb}} \right)^{b/3} \right]. \quad (3)$$

This quantity is rather complicated, depending explicitly on the initial jet energy (through ξ), average medium temperature, and average size of the medium. Also, it explicitly depends on centrality (through \bar{T} and \bar{L}_{Pb} , which decrease with increasing centrality), consistently with what is seen in Fig. 1. Furthermore, as centrality and initial energy of the

jet increase, ξ , \bar{T} , and \bar{L}_{Pb} become smaller, explaining why the ratio in Fig. 1 goes to 1 for high p_{\perp} and high centrality, which results in the problem of concealing the path-length dependence. Consequently, the ratio of R_{AA} s for different collision systems is not a suitable observable for extracting path-length dependence.

Suitable observable. It is clear that such an observable should expose coefficient b in a simplest possible manner. To initially gauge the appropriate functional dependence, we again resort to the scaling arguments given above for which we have shown to provide a reasonable description of the full-fledged numerical model results in Fig. 1. We proceed by subtracting R_{AA} s [obtained from Eq. (2)] from 1, which, in the case of Xe and Pb, reduces to

$$R_L^{XePb} \equiv \frac{1 - R_{XeXe}}{1 - R_{PbPb}} \approx \frac{\xi \bar{T}^a \bar{L}_{Xe}^b}{\xi \bar{T}^a \bar{L}_{Pb}^b} \approx \left(\frac{A_{Xe}}{A_{Pb}} \right)^{b/3}. \quad (4)$$

This new quantity R_L^{XePb} has a very simple form, which depends only on the medium size (through A_{Xe}/A_{Pb}) and on the path-length dependence, i.e., coefficient b , which is now directly exposed. Note again that this simple dependence is expected to hold for *higher centralities and higher initial p_{\perp}* where Eqs. (2) and (4) are applicable. Consequently, as one plots R_L^{XePb} at higher centrality regions, one may expect that this value will approach a limit that directly reflects the path-length dependence, i.e., relation given by Eq. (4).

To numerically test our proposal and assess the applicability of the analytically derived scaling in Eq. (4), we further concentrate only on higher centrality regions and calculate $(1 - R_{XeXe})/(1 - R_{PbPb})$ using our full-fledged numerical procedure [22]. This ratio is shown in Fig. 2; full, dashed, and dot-dashed curves show our full results for charged hadrons, D and B mesons, respectively; the dashed lines correspond to the $b = 1$ and 2 limits from Eq. (4). From Fig. 2, one can see that R_L^{XePb} is almost independent of centrality, which is exactly what one needs for such observable. At high- $p_{\perp} \rightarrow 100$ GeV, we clearly see that R_L^{XePb} for all types of particles reaches a limiting value as expected. Moreover, this limiting value ($R_L^{XePb} \approx 0.8$) directly reflects the underlying path-length dependence, which is, in our case (the dynamical energy-loss formalism with radiative and collisional energy

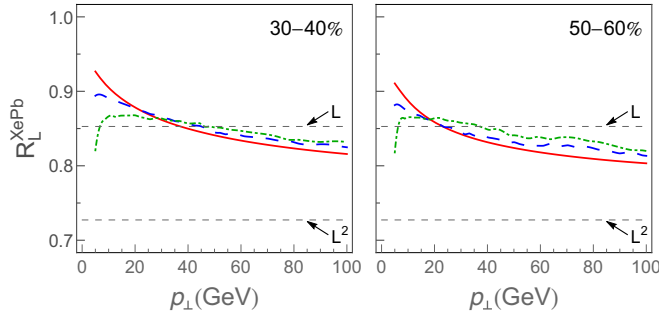


FIG. 2. Predictions for R_L^{XePb} as a function of p_\perp are shown for charged hadrons (full curves), D mesons (dashed curves), and B mesons (dot-dashed curves). Upper (lower) dashed gray lines correspond to the case in which energy-loss path-length dependence is linear (quadratic). Centrality regions are denoted in the upper right corners of each panel.

losses in a finite-size QCD medium), between linear and quadratic (i.e., $b \approx 1.4$), regardless of the particle flavor; note that this extracted path-length dependence is different from a common assumption of heavy flavor having linear, whereas light flavor having quadratic (LPM-like) dependence. It is, therefore, clear that, making such plots from experimental data and extracting the corresponding path-length dependence (exponent b), can be used to differentiate between different energy-loss models in a simple and direct manner. Also, note that, in distinction to Fig. 2, where the gray dashed lines are simple and intuitive (allowing straightforward inference of path-length dependence), defining such lines in Fig. 1 would not be possible.

Testing robustness and reliability. To address the robustness of the R_L^{AB} observable, i.e., if the observable is applicable to systems of diverse sizes, we further test R_L^{AB} on other smaller systems (Kr + Kr, Ar + Ar, and O + O). With this goal in mind, in Fig. 3, we concentrated on charged hadrons and generated full-fledged predictions for R_L^{AB} for Xe – Pb, Kr – Pb, Ar – Pb, and O – Pb as a function of p_\perp . From this figure, we first observe that, for all four systems, this observable is almost independent of centrality as expected from the arguments presented above. Second, we also observe that, independent of the collision system, this observable

shows the same behavior, so it is very robust with respect to extracting path-length dependence. We, moreover, observe that going to smaller systems makes extracting the path-length dependence even more straightforward since the separation between L and L^2 lines becomes larger when going to smaller systems, i.e., it increases for a factor of 2 when going from Xe – Pb to Ar – Pb and O – Pb. This then motivates using this observable across systems of different sizes and provides another argument for the utility of high- p_\perp measurements at the BSS at the LHC.

Finally, to address the reliability of this R_L^{AB} observable, in Fig. 3, we also show R_L^{AB} , calculated by using full numerical procedure stated above but if only collisional [5] (upper curves) or radiative [15] (lower curves) energy losses are taken into account—we here again concentrate on higher centrality regions where Eqs. (2) and (4) are applicable. Within the dynamical energy-loss model, collisional energy loss is close to—although somewhat less than—linear ($b \approx 0.9$) due to finite-size effects [5]. From Fig. 3, we see that this path-length dependence scenario is directly recovered where the approach to the appropriate dashed line (indicating $\lesssim L$ dependence) is almost ideal. For the radiative energy loss due to the LPM effect, path-length dependence approaches L^2 for higher p_\perp [15], and we see that, for such a scenario, R_L^{AB} also unambiguously recovers this tendency, although the spread of curves for different centralities is somewhat larger compared to the collisional energy-loss case. This, therefore, leads to the conclusion that, in addition to being simple and robust, R_L^{AB} is also an accurate observable for extracting path-length dependence.

Summary and outlook. Experimental measurements for smaller collision systems at the future BSS at the LHC will provide previously unprecedented opportunities to distinguish between different energy-loss mechanisms and, consequently, to better understand properties of created QGP. We here proposed a new—simple, robust, and reliable—observable for assessing the path-length dependence of the energy loss, which is a main signature of high- p_\perp parton-medium interactions. Based on our results, this observable can be used to straightforwardly extract the path-length dependence from experimental data, which can, consequently, be directly compared with such dependencies from various theoretical

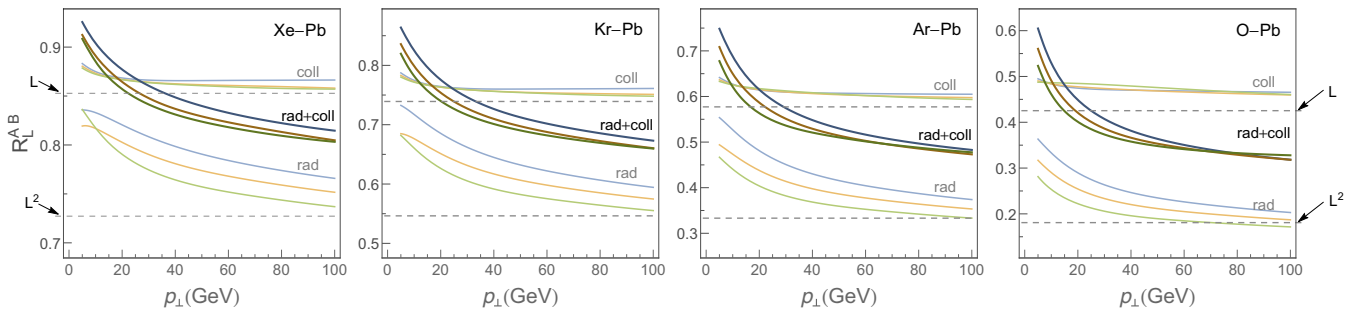


FIG. 3. Predictions for R_L^{AB} as a function of p_\perp are shown for charged hadrons where the darker sets of curves are obtained by using full dynamical energy loss, whereas upper and lower lighter sets or curves, respectively, correspond to the cases where only collisional or only radiative energy loss is considered. The first to fourth panels correspond to R_L^{XePb} , R_L^{KrPb} , R_L^{ArPb} , and R_L^{OPb} , respectively. In each panel, three centrality regions 30–40%, 40–50%, and 50–60% are marked by blue, orange, and green, respectively.

models as a major test of our understanding of energy-loss mechanisms.

Furthermore, our Rapid Communication also suggests that $(1 - R_{AA})$ might be a more suitable observable for the exploration of QGP than commonly used R_{AA} as we have here shown that it more directly reflects the underlying energy loss of the jet traversing the QGP. Furthermore, $(1 - R_{AA})$ observable appears to be highly correlated to v_2 (as noted in our recent study [41]). Since high- p_{\perp} observables are shown [41,42] to be sensitive to global QGP properties, we expect that including the full-medium evolution models (together with

event-by-event fluctuations) into the high- p_{\perp} predictions and providing a detailed joint study of high- p_{\perp} $(1 - R_{AA})$ and v_2 (and possibly higher harmonics) for different collision systems will prove to be an excellent tool for high-precision QGP tomography, which is a future major goal of relativistic heavy ion physics.

Acknowledgments. This work was supported by the European Research Council Grant No. ERC-2016-COG: 725741 and by the Ministry of Science and Technological Development of the Republic of Serbia under Projects No. ON171004 and No. ON173052.

-
- [1] J. C. Collins and M. J. Perry, *Phys. Rev. Lett.* **34**, 1353 (1975).
- [2] M. Gyulassy and L. McLerran, *Nucl. Phys. A* **750**, 30 (2005); E. V. Shuryak, *ibid.* **750**, 64 (2005); B. Jacak and P. Steinberg, *Phys. Today* **63**(5), 39 (2010).
- [3] J. D. Bjorken, FERMLAB-PUB-82-059-THY (1982).
- [4] JET Collaboration, K. M. Burke *et al.*, *Phys. Rev. C* **90**, 014909 (2014); Y. Xu *et al.*, *ibid.* **99**, 014902 (2019).
- [5] M. Djordjevic, *Phys. Rev. C* **74**, 064907 (2006).
- [6] M. H. Thoma and M. Gyulassy, *Nucl. Phys. B* **351**, 491 (1991); E. Braaten and M. H. Thoma, *Phys. Rev. D* **44**, R2625 (1991).
- [7] R. Baier, Y. L. Dokshitzer, A. H. Mueller, S. Peigne, and D. Schiff, *Nucl. Phys. B* **483**, 291 (1997); B. G. Zakharov, *JETP Lett.* **63**, 952 (1996).
- [8] N. Armesto, C. A. Salgado, and U. A. Wiedemann, *Phys. Rev. D* **69**, 114003 (2004).
- [9] P. B. Arnold, G. D. Moore, and L. G. Yaffe, *J. High Energy Phys.* **11** (2001) 057; **01** (2003) 030.
- [10] M. Gyulassy, P. Levai, and I. Vitev, *Nucl. Phys. B* **594**, 371 (2001).
- [11] X. N. Wang and X. F. Guo, *Nucl. Phys. A* **696**, 788 (2001); A. Majumder and M. Van Leeuwen, *Prog. Part. Nucl. Phys. A* **66**, 41 (2011).
- [12] C. Marquet and T. Renk, *Phys. Lett. B* **685**, 270 (2010); F. Dominguez, C. Marquet, A. H. Mueller, B. Wu, and B. W. Xiao, *Nucl. Phys. A* **811**, 197 (2008).
- [13] C. A. G. Prado, J. Noronha-Hostler, R. Katz, A. A. P. Suaide, J. Noronha, and M. G. Munhoz, *Phys. Rev. C* **96**, 064903 (2017).
- [14] M. Nahrgang, J. Aichelin, P. B. Gossiaux, and K. Werner, *Phys. Rev. C* **93**, 044909 (2016).
- [15] M. Djordjevic, *Phys. Rev. C* **80**, 064909 (2009); M. Djordjevic and U. Heinz, *Phys. Rev. Lett.* **101**, 022302 (2008).
- [16] B. Betz and M. Gyulassy, *J. High Energy Phys.* **08** (2014) 090; **10** (2014) 043(E).
- [17] J. Noronha-Hostler, B. Betz, M. Gyulassy, M. Luzum, J. Noronha, I. Portillo, and C. Ratti, *Phys. Rev. C* **95**, 044901 (2017).
- [18] B. Blagojevic and M. Djordjevic, *J. Phys. G: Nucl. Part. Phys.* **42**, 075105 (2015).
- [19] T. Renk, *Phys. Rev. C* **85**, 044903 (2012); D. Molnar and D. Sun, *Nucl. Phys. A* **932**, 140 (2014); **910**, 486 (2013).
- [20] D. Zigic, I. Salom, M. Djordjevic, and M. Djordjevic, *Phys. Lett. B* **791**, 236 (2019).
- [21] T. Renk, H. Holopainen, J. Auvinen, and K. J. Eskola, *Phys. Rev. C* **85**, 044915 (2012).
- [22] D. Zigic, I. Salom, J. Auvinen, M. Djordjevic, and M. Djordjevic, [arXiv:1805.03494](https://arxiv.org/abs/1805.03494) [*J. Phys. G: Nucl. Part. Phys.* (to be published)].
- [23] J. I. Kapusta, *Finite-Temperature Field Theory* (Cambridge University Press, Cambridge, UK, 1989).
- [24] M. Djordjevic and M. Djordjevic, *Phys. Lett. B* **709**, 229 (2012).
- [25] M. Djordjevic and M. Djordjevic, *Phys. Lett. B* **734**, 286 (2014).
- [26] B. Blagojevic, M. Djordjevic, and M. Djordjevic, *Phys. Rev. C* **99**, 024901 (2019).
- [27] Z. B. Kang, I. Vitev, and H. Xing, *Phys. Lett. B* **718**, 482 (2012); R. Sharma, I. Vitev, and B. W. Zhang, *Phys. Rev. C* **80**, 054902 (2009).
- [28] M. Gyulassy, P. Levai, and I. Vitev, *Phys. Lett. B* **538**, 282 (2002).
- [29] A. Dainese, *Eur. Phys. J. C* **33**, 495 (2004).
- [30] D. de Florian, R. Sassot, and M. Stratmann, *Phys. Rev. D* **75**, 114010 (2007); M. Cacciari and P. Nason, *J. High Energy Phys.* **09** (2003) 006.
- [31] M. Djordjevic and M. Djordjevic, *Phys. Rev. C* **92**, 024918 (2015).
- [32] M. Djordjevic, *Phys. Lett. B* **763**, 439 (2016).
- [33] S. Acharya *et al.* (ALICE Collaboration), *J. High Energy Phys.* **11** (2018) 013.
- [34] V. Khachatryan *et al.* (CMS Collaboration), *J. High Energy Phys.* **04** (2017) 039.
- [35] J. Xu, A. Buzzatti, and M. Gyulassy, *J. High Energy Phys.* **08** (2014) 063.
- [36] G. Giacalone, J. Noronha-Hostler, M. Luzum, and J. Y. Ollitrault, *Phys. Rev. C* **97**, 034904 (2018).
- [37] C. Loizides, J. Kamin, and D. d'Enterria, *Phys. Rev. C* **97**, 054910 (2018).
- [38] K. J. Eskola, H. Niemi, R. Paatelainen, and K. Tuominen, *Phys. Rev. C* **97**, 034911 (2018).
- [39] S. Acharya *et al.* (ALICE Collaboration), *Phys. Lett. B* **790**, 35 (2019).
- [40] A. M. Sirunyan *et al.* (CMS Collaboration), *J. High Energy Phys.* **10** (2018) 138.
- [41] M. Djordjevic, S. Stojku, M. Djordjevic, and P. Huovinen, [arXiv:1903.06829](https://arxiv.org/abs/1903.06829).
- [42] C. Andres, N. Armesto, H. Niemi, R. Paatelainen, and C. A. Salgado, [arXiv:1902.03231](https://arxiv.org/abs/1902.03231).